IEEE Access
Multidisciplinary ⋮ Rapid Review ⋮ Open Access Journal

Received 13 May 2023, accepted 2 June 2023, date of publication 6 June 2023, date of current version 12 June 2023.

Digital Object Identifier 10.1109/ACCESS.2023.3283297

RESEARCH ARTICLE

Implementation of New Optimal Control Methodology of Quazi Z-Source Inverter Based on MPC

MOHAMED A. ISMEIL[1,2], (Member, IEEE), OMAR ABDEL-RAHIM[3,4], (Senior Member, IEEE), HANY S. HUSSEIN[1,3], (Senior Member, IEEE), AND ESAM H. ABDELHAMEED[3]

[1]Electrical Engineering Department, Faculty of Engineering, King Khalid University, Abha 61411, Saudi Arabia
[2]Electrical Engineering Department, Faculty of Engineering, South Valley University, Qena 83523, Egypt
[3]Electrical Engineering Department, Faculty of Engineering, Aswan University, Aswan 81528, Egypt
[4]Department of Electrical Power Engineering, Egypt-Japan University of Science and Technology (E-JUST), Borg El-Arab, Alexandria 21934, Egypt

Corresponding authors: Omar Abdel-Rahim (O.abdelrahim@aswu.edu.eg) and Esam H. Abdelhameed (ehhameed@energy.aswu.edu.eg)

This work was supported by the Deanship of Scientific Research, King Khalid University, Abha, Saudi Arabia, through General Research Project, under Grant GRP.2/162/44.

ABSTRACT Model predictive control (MPC) is a well-known control methodology in power electronics systems, due to its ability to deal with the system's nonlinearities and superior dynamic response. MPC is able to handle multiple variables by adjusting the cost function, but this leads to high computational costs, especially for systems having a big number of switches. This problem increases when not only performance efficiency is required but also minimizing the power losses of these systems. In this paper, a modified MPC algorithm is presented for controlling a three-phase quasi Z-source inverter (qZSI), i.e., providing switching states to be applied for qZSI control, so that, within less computation time, total harmonic distortion (THD) of the output currents is maintained at the minimum level with concurrent minimization of inverter switch power losses. The computational burden is reduced by using calculation loop optimization, reducing the number of switching states in the loop and unrolling the calculation loop. To highlight the effectiveness of the proposed control methodology, a numerical simulation was carried out using MATLAB software. The obtained results have been discussed and compared with those of a recent previous study.

INDEX TERMS Model predictive control (MPC), quasi Z-source inverter (qZSI), switching losses, conduction losses, total harmonic distortion (THD).

I. INTRODUCTION

Given the global energy crisis, many countries have planned to benefit from renewable energies, especially wind and photovoltaic energy. Statistics show that the consumption of renewable energy increased by 2.9 EJ, with an annual growth rate of 9.7% over 10 years, reaching a peak in 2020 [1]. However, connecting these sources to the electrical grid or different loads poses several challenges. Some researchers proposed solutions such as using a large transformer to interface the AC voltage after the inverter and the grid or AC loads [2], [3]. This system has drawbacks such as the high cost and size of the transformer, and the limitations of the voltage level and power rating of the inverter. Another solution is to use a two-stage converter [4], [5], where the first stage steps up the DC voltage and the second stage inverts it to AC voltage. But this also increases the cost and complexity of the control circuit and components. To overcome these problems, some researchers suggested using single-stage converters without transformers, based on new topologies called multi-level inverters [6], [7], [8], [9], [10]. These inverters use many power devices connected by passive and active switches, which require complex control circuits. A different approach is to use a single-stage converter without a transformer and without any extra active switch., this new topology is called Z-Source Inverter (ZSI) shown in Fig. 1. The theory of

The associate editor coordinating the review of this manuscript and approving it for publication was Alexander Micallef.

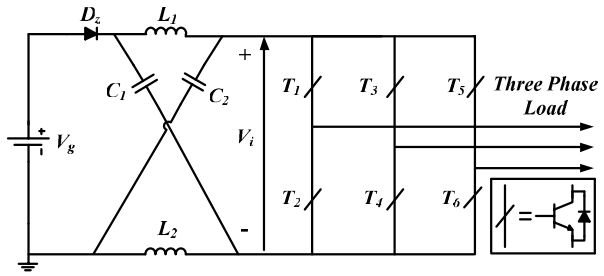

FIGURE 1. Classical Z-source inverter (ZSI) topology.

operation is based on introducing the nine-state, to be added to the eight cases that existed before by making two switches turn on at the same moment for one leg [11], [12].

ZSI has some advantages, but it also has some problems. For example, it puts stress on the capacitors and switches, and it works in Discontinuous Conduction Mode (DCM). To solve these problems, the quazi Z-Source inverter (qZSI) shown in Fig. 2 was introduced. The qZSI works in Continuous Conduction Mode (CCM) and reduces the stress on the relays and switches [13], [14], [15].

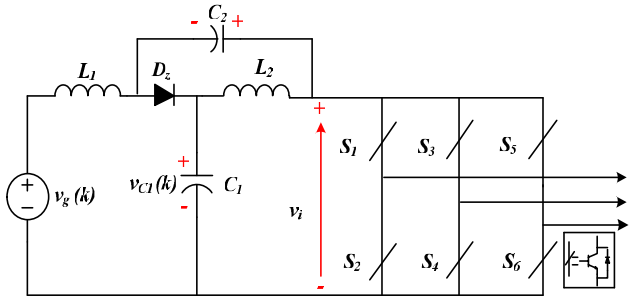

FIGURE 2. Structure of quasi ZSI topology.

The qZSI has attracted a lot of research interest in improving its performance, both in terms of the power circuit [16], [17] and the control strategies [18], [19]. The development of the power circuit led to an increase in the boost factor. On the control side, the use of the model predictive controller (MPC) led to an increase in the dynamic response performance for qZSI. For the qZSI operation, the switch states can be selected by an optimized control based on MPC, which can overcome many problems of the qZSI inverter. This is what we will focus on in this paper. In recent years, several works have proposed the use of Finite Control Set Model Predictive Control (FCS-MPC) to control various types of power converters and electrical drives [20]. The main advantages of this control technique are its conceptual simplicity, its easy implementation, its ability to handle non-linearities, and its ability to control multiple variables with a single structure and fast dynamic response. FCS-MPC explicitly considers the power switches as a constraint in the optimal problem, therefore it is necessary to consider all possible states of the converter in the implementation of the algorithm. FCS-MPC requires that the optimization problem be solved online. This involves a large number of calculations, becoming a drawback for its implementation in standard control hardware platforms [21], [22], [23], [24], [25], [26], [27], [28], [29], [30]. In [21] a delay compensation strategy is designed to compensate for the time delay between the sampling time and switching time. Also, a Kalman observer is established to compensate for the current reference and modify the predictive model. In addition, a disturbance suppression method is proposed. The main challenge is the heavy computation that results from the objective function optimization at each switching time. Moreover, the random selection of the switching states may cause undesirable effects such as high switching frequency and harmonic distortion, on the other hand, this control is not suitable for power factor correction [22]. In [23] the proposed control used only FCS-MPC, which achieved three control objectives with only one cost function: the dc-link voltage regulation, and the active and reactive power injected into the main grid. Using this algorithm led to an increase in the switching frequency of the inverter based on variable switching frequency (VSF), hence the losses increased due to the higher switching frequency [24]. In [25] a dual active bridge was used based on MPC. Moreover, the control considered the large signal stability and all calculations were done under the assumption of a large-scale system, which added to the cost function. In [26] the current stress was optimized based on MPC with triple phase shift (TPS) modulation. However, this method required a lot of time-consuming work with complicated computation [27]. The computational cost of FCS-MPC depended on the algorithm used to solve the optimization problem. Additionally, FCS-MPC had a high computational cost when it was implemented in an advanced multilevel topology like the Flying Capacitor Converter (FCC) [28]. In [28], a fast FCS-MPC imitator was proposed based on two shallow artificial neural networks (SANNs) that were implemented sequentially. The proposed control method was implemented for a grid-tied three-level neutral point clamped power converter. Compared to the existing ANN-based approaches, this control technique allowed much reduction in the number of neurons in hidden layers.. This indicates that the computational complexity is much lower than both FCS-MPC and ANN-MPC while achieving similar control performance. In this article, simultaneous THD reduction and switching power loss minimization are targeted within less computation time based on loop optimization. This means increasing execution speed and reducing the overheads associated with loops. This has been done via the loop unrolling technique, in which the iterations of the optimization process are reduced. The studies [29], and [30] introduced methodologies for controlling power electronics aiming to improve MPC performance using artificial neural network (ANN). In [29], a control method for a two-level converter was introduced that combined MPC and ANN to produce a high-quality voltage with low total harmonic distortion (THD). However, to reduce the MPC calculation time during solving the optimization problem, the authors first used MPC to generate the required

data for training an ANN off-line. Then, this ANN was used online for voltage tracking purposes instead of using the MPC strategy.

In order to reduce the impact of parameter uncertainties while controlling power electronics such as a three-phase four-level flying capacitor inverter, an ANN-based model-free control strategy was introduced in [30]. The designed control scheme provided better inverter performance and improved the system's robustness against parametric uncertainties, in comparison with the traditional MPC approach. The authors of [31] proposed an ANN-MPC technique to avoid the computational complexity of the conventional MPC. First, they designed a virtual MPC controller to provide a database that was used to train an ANN offline. Then, they designed an actual FPGA-based MPC controller that utilized the trained ANN to control the real-time operation of the power converter instead of using a heavy-duty mathematical computation MPC scheme. The designed ANN-MPC successfully reduced the FPGA resource requirements. In [32], the authors introduced an ANN-based FCS-MPC imitator (ANN-MPC) that took advantage of the parallel computing feature of the ANN to control a neutral point clamped converter. The designed controller provided better control performance and a significant reduction in the computation resource requirement.

This study has modified a model predictive control (MPC) algorithm [33], that was used to control a three-phase quasi Z-source inverter (qZSI) by providing the switching states of the inverter. The original MPC algorithm aimed to minimize the total harmonic distortion (THD) of the output currents without considering the inverter power losses. The modified MPC (MMPC) algorithm has been proposed to simultaneously minimize the THD of the inverter output current and the switching and conduction losses of the inverter switches within a shorter computation time. Usually, an optimization technique can be applied to achieve the control objectives. In this research, the best candidate optimization algorithm has been used to find a set of qZSI switching states that can optimize the objective function by minimizing a specific cost function. Moreover, to reduce the computation time to obtain the optimal solution, the authors have replaced the cost function with two functions: the main cost function and the sub-cost function. The main cost function is based on the MPC methodology that minimizes the THD for improving the performance efficiency, while the sub-cost function tests the zero and shoot-through states for selecting a candidate solution among their alternatives that can reduce the qZSI power losses. Therefore, an optimized operation strategy based on the best candidate optimization algorithm has been proposed to adjust the qZSI switches and ensure concurrent minimization of THD and qZSI power losses within a reasonable computation time. The paper is organized as follows: Section II presents the modified model predictive control, Section III presents the proposed model predictive control, and Section IV presents the simulation results.

II. MODIFIED MODEL PREDICTIVE CONTROL (MMPC)

The three-phase voltage source inverter (VSI) can connect the three-phase load to the positive or negative terminals of the DC link (V_{dc}) by using different combinations of their switches. However, qZSI has an extra state in addition to the eight states, which is a shoot-through state [33]. This study proposes a modified model predictive controller (MMPC) as shown in Fig. 3 to achieve its control objectives by expanding the switching states of qZSI. Therefore, 15 possible switching states are suggested for qZSI as shown in Table 1 instead of 9 states in [33]. These states include two zero states ($V_1 : V_2$), six active states ($V_3 : V_8$) and seven shoot-through states ($V_9 : V_{15}$). As shown in Table 1, each active state has only one option among ($V_3 : V_8$) (the active states are not interchangeable). However, there are multiple switching options for the zero and shoot-through states. For the zero states, one can choose between ($V_1 : V_2$) and for the shoot-through states, one can choose among ($V_9 : V_{15}$) To compromise between getting the two objectives of the MMPC, the first objective (which is the reduction of the output current THD) can be obtained via selecting the switching case i.e. active, zero, or shoot-through case. However, the second objective (which is qZSI power losses minimization) can be obtained through selecting the best state among the alternatives of each switching case. This methodology is discussed in details in Section III.

Commonly, for a predictive controller, the prediction horizon which is the number of future control intervals in the controller should be chosen. Practical studies have proven that it is better to choose the prediction horizon early in the design of the predictive controller and to keep it constant. Moreover, the trend is to adjust the other elements in the cost function. Therefore, in this article, the prediction horizon in the MPC has been chosen from the first degree to speed up the tuning process.

Finally, the modeling methodology of qZSI under the proposed MMPC has been obtained in three stages; the first one predicts the space vector of the output voltage across the load, the second stage creates the model of output load, whereas the prediction equations of the capacitor and inductor in different operation modes of the qZSI have been given in the final stage. The following subsections discuss the three stages of the qZSI modeling.

A. THE SPACE VECTOR OF THE OUTPUT VOLTAGE ACROSS THE LOAD

The space vector of the output voltage across the load $V_i(k+1)$ for the iteration i where $i = [0{:}7]$, are estimated using the switching states and the peak value of the DC link voltage (V_{dc}) as follows:

$$V_i(k+1) = \frac{2.V_{dc}}{3} \quad (S_a + a.S_b + a^2.S_c) \tag{1}$$

where S_a, S_b and S_c are the switching states for phases a, b, and c; respectively, (either 0 or 1). The space vector for all possible switching sates is shown in Fig. 4.

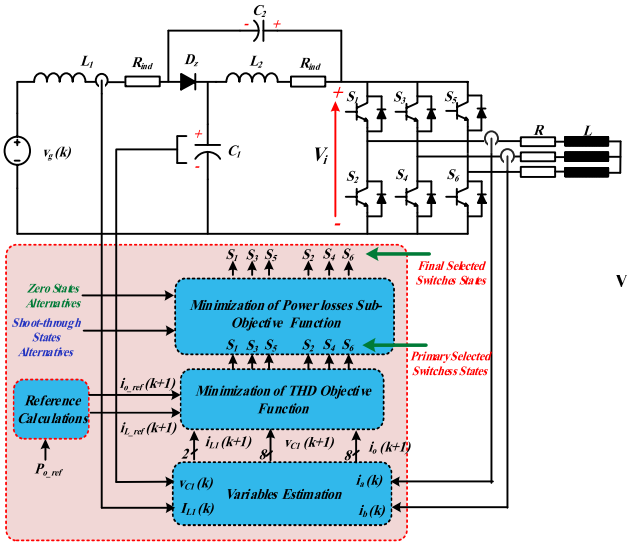

FIGURE 3. Schematic diagram of the modified MPC-based control methodology.

TABLE 1. Possible switching states of qZSI and its space output voltage.

State #	qZSI Switching States						Case	Output Voltage
	S_1	S_3	S_5	S_2	S_4	S_6		
1	OFF	OFF	OFF	ON	ON	ON	Zero	$V_0 = 0$
2	ON	ON	ON	OFF	OFF	OFF		
3	ON	OFF	OFF	OFF	ON	ON	Active	$V_1 = \frac{2}{3}.V_{dc}$
4	ON	ON	OFF	OFF	OFF	ON		$V_2 = \frac{1}{3}.V_{dc} + j.\frac{\sqrt{3}}{3}.V_{dc}$
5	OFF	ON	OFF	ON	OFF	ON		$V_3 = -\frac{1}{3}.V_{dc} + j.\frac{\sqrt{3}}{3}.V_{dc}$
6	OFF	ON	ON	ON	OFF	OFF		$V_4 = -\frac{2}{3}.V_{dc}$
7	OFF	OFF	ON	ON	ON	OFF		$V_5 = -\frac{1}{3}.V_{dc} - j.\frac{\sqrt{3}}{3}.V_{dc}$
8	ON	OFF	ON	OFF	ON	OFF		$V_6 = \frac{1}{3}.V_{dc} - j.\frac{\sqrt{3}}{3}.V_{dc}$
9	ON	ON	OFF	ON	ON	OFF	Shoot-Through	$V_7 = 0$
10	OFF	ON	ON	OFF	ON	ON		
11	ON	OFF	ON	ON	OFF	ON		
12	OFF	OFF	ON	OFF	OFF	ON		
13	OFF	ON	OFF	OFF	ON	OFF		
14	ON	OFF	OFF	ON	OFF	OFF		
15	ON	ON	ON	ON	ON	ON		

B. LOAD CURRENT

The predictive value of load current $i_o(k+1)$, can be calculated from the value of output voltage as:

$$i_o(k+1) = \frac{T_s.V_i(k+1) + L.i_o(k)}{L + R.T_s} \tag{2}$$

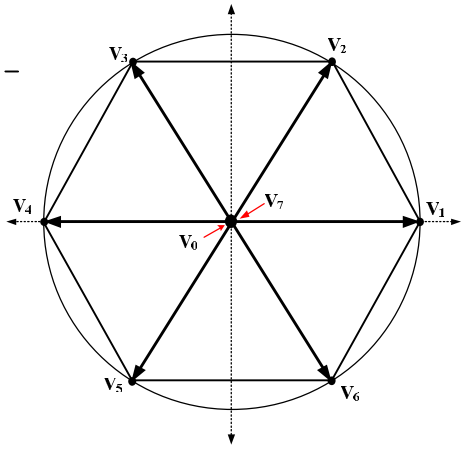

FIGURE 4. Space vectors of output load voltage based on switching states.

where: $i_o(k)$ load current at (k) instant, T_s, R and L are the sampling period, the resistance, and the inductance of the RL load respectively.

C. THE INDUCTOR CURRENT AND CAPACITOR VOLTAGE

To simplify the analysis, we consider that the inductors and capacitors have the same value. We also assume that the system operates in CCM and neglect the ESR of both capacitors since it is very small. The qZSI has two operating modes, which are described below:

1) NON SHOOT-THROUGH MODE

The action of this mode can be applied when any of the six active switchings occurs. the equivalent circuit in this mode is shown in Fig. 5

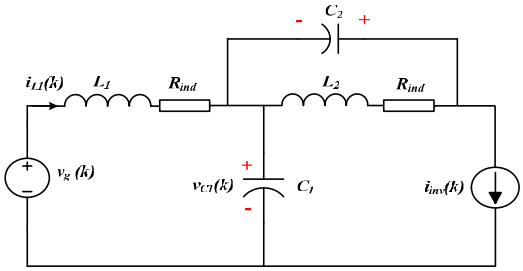

FIGURE 5. Equivalent circuit of qZSI at the non-shoot-through case.

The relations between both inductor current I_{L1} and capacitor voltage V_{C1} can be expressed as:

$$L_1.\frac{di_{L1}(k)}{dt} = v_{C1}(k) - v_g(k) + R_{ind}.i_{L1}(k) \tag{3}$$

$$C_1.\frac{dv_{C1}(k)}{dt} = i_{L_1}(k) - i_{inv}(k) \tag{4}$$

where, C_1, L_1 are the capacitance and inductance for the qZSI passive network R_{ind} is the internal resistance of the inductor for qZSI, $v_g(k)$ is the input voltage, $i_{inv}(k)$ is the inverter output current. $v_{C1}(k)$ is the capacitor voltage, and $i_{L_1}(k)$ is the inductor current at (k) instant.

The predictive inductor current $i_{L_1}(k+1)$ and the predictive capacitor voltage $v_{C_1}(k+1)$ can be driven from (3), (4) as:

$$i_{L_1}(k+1) = \frac{T_s.(v_g(k) - v_{C_1}(k)) + L_1.i_{L_1}(k)}{L_1 + R_{ind}.T_s} \quad (5)$$

$$v_{C_1}(k+1) = v_{C_1}(k) + \frac{T_s}{C_1}(i_{L_1}(k+1) - i_{inv}(k+1) \quad (6)$$

2) SHOOT-THROUGH CASE

During this mode, the capacitors C_1, C_2 are discharged across the two inductors L_1, L_2 as shown in Fig. 6

$$L_1.\frac{di_{L1}(k)}{dt} = v_{C1}(k) - v_g(k) + R_{ind}.i_{L1}(k) \quad (7)$$

$$C_1.\frac{dv_{C1}(k)}{dt} = i_{L_1}(k) - i_{inv}(k) \quad (8)$$

In the same way, the predicted values in (7), (8) can express as:

$$i_{L_1}(k+1) = \frac{T_s.v_{C_1}(k) + L_1.i_{L_1}(k)}{L_1 + R_{ind}.T_s} \quad (9)$$

$$v_{C_1}(k+1) = v_{C_1}(k) - \frac{T_s}{C_1}i_{L_1}(k+1)\,(10) \quad (10)$$

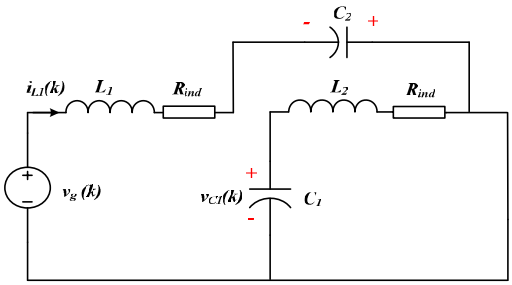

FIGURE 6. Equivalent circuit of qZSI at the shoot-through case.

III. PROPOSED OPTIMIZATION METHODOLOGY

As the effectiveness of the MPC scheme depends mainly on the computation time, therefore to achieve minimum computational effort of the MPC algorithm, a modified methodology of [27] has been applied i.e. the authors have utilized a modified algorithm in which, to avoid passing through excessive calculation loop, zero and shoot-through cases are represented by only one predefined state for each case while neglecting the other states that represents zero and shoot-through cases, accordingly, although the original set of candidates includes 15 states representing all the applicable states for qZSI switching, only 8 states have been used in this stage as a reduced set of candidates, from which the optimal solution of THD problem is generated. That set includes six states for representing the active case, one states for representing the zero state case, and one state for representing the shoot-through case. On the other hand, for solving the qZSI power losses issue, when the zero or shoot-through state provides a minimum value of the main cost function, the algorithm must pass through another iterative process for selecting the optimized states among the zero or shoot-through alternatives. The power losses minimization can be obtained as the switches are only switched when it is needed to the state of minimum switching and conduction losses. This process includes a little repetition of the calculation which is one repetition in case of zero case and six repetitions in the case of shoot-through case. The key feature of the proposed methodology is that qZSI has been optimally controlled based on an iterative scenario within a restricted time horizon through reducing the computation time of the main and sub-cost functions, which are responsible for optimizing the THD ratio (performance efficiency) and qZSI power losses, respectively. The calculation time of the main cost function can be saved by 46.67%. However, the computation time of the sub-cost function can be reduced for active case, zero case, and shoot-through case by 100%, 93.33%, and 60%, consecutively.

This study is meant to minimize the THD of the output current and the qZSI power losses, i.e. switching and conduction losses, when using an MPC algorithm. The procedure of the proposed optimization-based MPC methodology for solving this problem is described in Algorithm 1 as a pseudo-code form. The following procedure is repeated at each sample time in the MPC program implementation: As illustrated in the pseudo-code algorithm the proposed control methodology is an iterative optimization process that has been done through three stages as follows: the 1st stage includes preparation (definition and/or prediction) of the required data (system parameters and variables) for the second stage, i.e. the peak value of the DC link voltage, the reference of the load current, the capacitor voltages, load currents, drain-source voltages, and the drain currents are defined, where switches currents and voltages are estimated based on (5) & (6). As a modified optimization strategy, the switches states are defined in Fig. 3 and Table 1 in three sets, the first set is called (***AZSset***) which expresses the active, zero, and shoot-through states as defined by [20] while the optimal switching state was selected among eight states i.e. one zero state, six active states, and one shoot-through state. In this study, the elements of ***AZSset*** have been set as {state #1, states #3-8, state #15} which have indices from 1 to 8. The second and third sets of switching states are called (***ZSset***) and (***SSset***) which express all possible alternatives of the zero, and shoot-through states, respectively. In order to improve computing efficiency within less computation time, this research divides the optimization into two sub-problems in terms of THD and qZSI power losses which are implemented through the 2nd and the 3rd stages. The 2nd stage has been designed to optimize the total harmonic distortion (THD) of the output current based on a modified version of the MPC technique introduced by [20]. Throughout this stage one qZSI switching state x_{opt} should be chosen (called THD optimal state) among the states of ***AZSset*** relying on minimizing cost function $g(x)$, where:

$$g(x) = \alpha \cdot \left(\left|Re\left(i_{k_{ref}} - i_{k1}\right)\right| + \left|Im\left(i_{k_{ref}} - i_{k1}\right)\right|\right) + \beta \cdot |V_{dc} - V_{c1}|) + \gamma \cdot \left|I_{L\_ref} - I_{L1}\right| \quad (11)$$

where $i_{k_{ref}}$ is the reference current for the output load, and i_{k1} is the predictive current for the output load V_{cref} is the reference value of the capacitor voltage and its average value equals the Vdc, It is worth noting that, β, and γ are weighting factors, and these values are the means of tuning the algorithm of the MPC, and they depend primarily on choosing values so that the largest value gives priority to the variable to be controlled. From another point of view, weighting factors are an indirect way to achieve normalization between the variable to be controlled. The values of α, β, and γ have been chosen as 1.8, 1.75, and 40.0, respectively by try and error way. I_{L_ref} is the reference inductor current for qZSI network and I_{L1} is the predictive value of the inductor current for qZSI network The functions $Re(\cdot)$ and $Im(\cdot)$ are used to calculate the real and imaginary components, respectively. Minimization of g (i) can be achieved in an online manner by designing the optimization algorithm to generate the qZSI switching set each sampling period. Moreover, as the total switches power losses (P_{loss}) in any component operating in the switch mode can be obtained as the sum of the switching losses (P_{sw}) and conduction losses (P_C) of that component, therefore, P_{loss} of qZSI when applying the selected state can be calculated using the following equations:

$$P_{loss} = P_{sw} + P_C \tag{12}$$

$$P_{sw} = \left(E_{on} + E_{off}\right).f_{sw} \tag{13}$$

$$P_C = R_{DSon} \cdot I^2_{\text{Drms}} \tag{14}$$

where E_{on} and E_{off} are the turn-on and turn-off energy losses in the MOSFET switch, respectively, f_{sw} is the switching frequency, R_{DSon} is the drain-source on-state resistance, and I_{Drms} is the rms value of the MOSFET on-state current. During the 3rd stage as the switches power losses calculation in case of zero and shoot-through states is considered an iteration-independent branch of the main optimization problem, there might be some benefit from unrolling the switches power losses loop for reducing the iterations of the optimization process (loop optimization) then this loop will be conditionally executed. Thus, the alternative sets of zero and shoot-through states, i.e. ZSset and SSset, will be tested in a conditional execution loop to guarantee getting minimum power losses of qZSI depending on minimizing a sub-cost function P_{loss} (i) which is defined by (12). The final optimal state is obtained according to which state has the least power losses; the THD optimal state or the alternative one i.e. the transistors are switched to a state that keeps qZSI switches power losses at the minimum level. The previous optimization procedure calculation has been done within a finite time horizon (sampling time) of 15 μsec.

Algorithm 1 Modified MPC-Based qZSI Control Methodology

THD & qZSI power losses minimization based on MPC
Procedure
  Measure the current values of V_{C1}, I_a, I_b, I_{L1}
  Define system parameters and ***AZSset***
  Initialize
  the optimal main objective function $g_{opt} = \infty$
  optimal state index $inx_{opt} = 0$
  for all element x of ***AZSset*** **do**
    if index of the previous x equal 8 **then**
      Use Eqs. (9) & (10) to predict the values of V_{C1} & I_{L1}
    else
      Use Eqs. (5) & (6) to predict the values of V_{C1} & I_{L1}
    end if
    Calculate main objective function $g(x)$ from Eq. 11
    if $g(x) < g_{opt}$ **then**
      $g_{opt} = g(x)$, $inx_{opt} = i$, $x_{opt} = AZSset(i)$
    end if
  end for
  if $inx_{opt} = 8$ **then**
    raise shoot-through case flag
  elseif $inx_{opt} = 1$ **then**
    raise zero case flag
  end if
  Set the THD optimal state is x_{opt}
  Calculate total power losses (P_{loss_opt}) using Eqs. (12):(14)
  if shoot-through case flag raised **then**
    for all element x of ***SSset*** **do**
    Calculate sub-cost function (P_{loss}) using Eqs. (12):(14)
    if $P_{loss} < P_{loss\_opt}$ **then**
      $P_{loss\_opt} = P_{loss}$, $x_{opt} = SSset(i)$
    end if
    end for
  elseif zero case flag raised **then**
    for all element x of ***ZSset*** **do**
    Calculate sub-cost function (P_{loss}) using Eqs. (12):(14)
    if $P_{loss} < P_{loss\_opt}$ **then**
    $P_{loss\_opt} = P_{loss}$, $x_{opt} = ZSset(i)$
    end if
    end for
  end if
  Set the THD & qZSI Power losses final optimal state is x_{opt}
end procedure

IV. RESULTS AND DISCUSSION

The proposed algorithm has been validated based on MATLAB SIMULINK software and the parameters used have listed in Table 2.

As discussed in section III, to achieve the losses objective of qZSI, the proposed optimization methodology of the MMPC is based on expanding the number of the checked switching states from 9 states in [33] to 15 states in the proposed scheme, accordingly, the number of For-Loops

TABLE 2. The Parameters of the qZSI topology under the proposed algorithm.

Parameter	Label	Value
Input voltage	V_g	40V
SL-qZSI network	$L_1 = L_2 = L_3$	500µH
	$C_1 = C_2$	470 µF
Internal resistance of Inductor	R_{ind}	5 mΩ
Sampling Time	T_s	10 µSec

which is used to select the optimal operating switching state should be increased resulting in increasing the computation time. However, in this study, the computational burden has been reduced by utilizing calculation loop optimization by reducing the number of switching states in the loop and calculation loop unrolling. The number of switching states has been reduced in the main optimization loop by selecting one state among the ***AZSset*** this reduces the number optimization loops by 46.67% as the state number is reduced from 15 states to 8 states only. Moreover, the qZSI losses objective is achieved through testing a sub-cost function via additional For-Loops in case of zero and shoot-through switching cases, however, there is no need for testing this sub-cost function in case of the active switching case. In case of selecting a zero state in the main THD loop, only one additional state should be tested whereas 6 states should be tested in case of selecting a shoot-through state in the main THD loop. A summary of the time reduction due to the proposed scheme is shown in Table 3 which indicates that the proposed methodology is able to reduce the computation time successfully with a total average time of 56.0% assuming equal probability for the three switching state cases.

TABLE 3. Computation time reduction due to the proposed scheme.

Switching Case		Main cost function THD minimization	Sub-cost function qZSI power losses reduction	Average
State #		8 States of 15 States	7 States of 15 States	
Computation Time Reduction	Active 6 states	46.67% Loop for 8 states Save 7 of 15	100% Save 7 of 7	71.56%
	Zero 2 states		85.71% Save 6 of 7	64.89%
	Shoot-through 7 states		14.29% Save 1 of 7	31.56%
Total Average (assume equal probability for the three state Cases)		--	--	56.0%

Two cases of studies are considered for comparative purposes, between the proposed technique and the MPC technique presented in [33] based on change the AC load. In case study #1, (1Ω + 10mH) RL load and power change from 150W to 300W are considered with a step change in the power at t=0.303s. And in case study, #1, (12Ω + 5mH) RL load and power change from 150W to 500W are considered with a step change in the power at t = 0.303s. Switches power losses of the system under both techniques are presented in FIGURE 7 and 8. Looking at the switches power losses of the system under both techniques, it is clear that the proposed algorithm has much lower switches power losses. Overall system efficiency of the system has been improved by 20% in case study #1 and around 22.5% in case study #2 after implementing the proposed minimum loss algorithm.

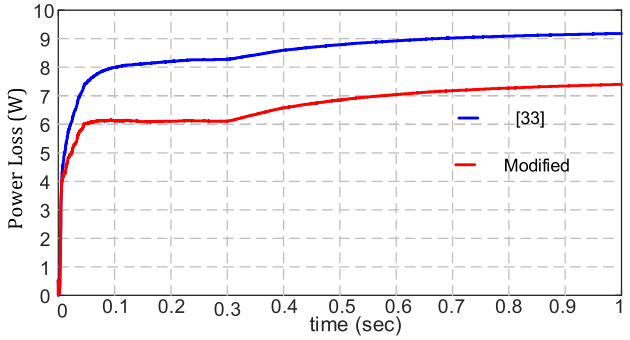

FIGURE 7. Switches power losses comparison for case study #1 using the MPC technique introduced in [33] and the proposed MMPC.

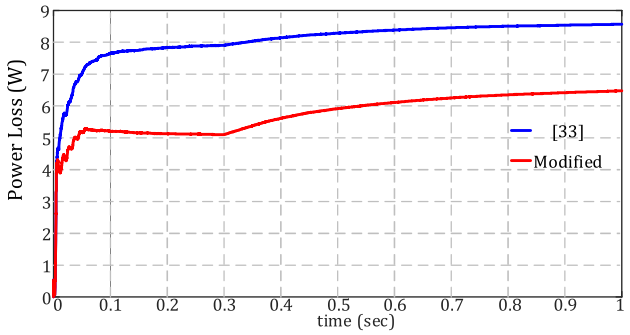

FIGURE 8. Switches power losses comparison for case study #2 using the MPC technique introduced in [33] and proposed MMPC.

Though the proposed algorithm focuses on switching loss minimization, it is designed to maintain total harmonic distortion (THD) and transient performance within the acceptable range. Figures 9 and 10, are the system performance for technique [33] and the proposed technique for case study #1, respectively. In both cases of study, the two techniques are able to track the reference current and fix capacitors voltages at 120V for V_{c1} and 50V for V_{c2}. In addition, in the proposed technique for case study #1 due to the increase in the number of calculations, the performance response to the reference exceeded to be five milliseconds, while [33] provided a quick response compared to the proposed technique where it was able to follow the reference in less than

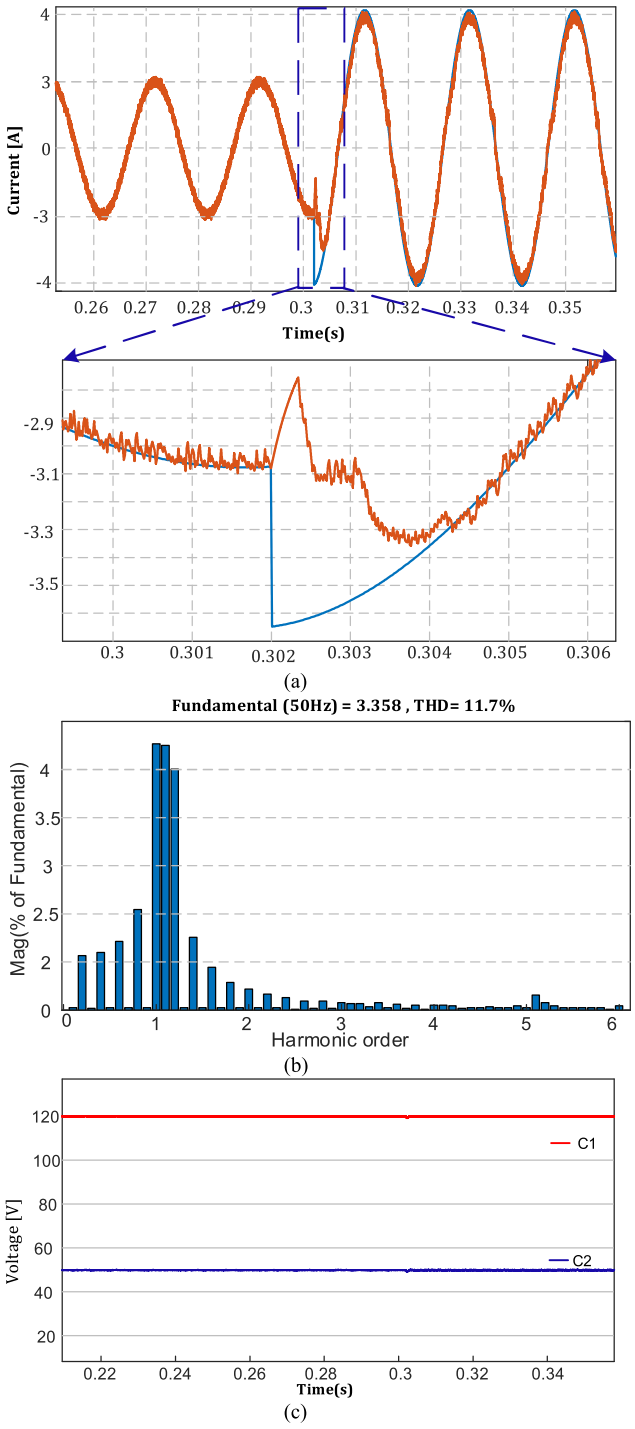

FIGURE 9. Case study #1 using MPC technique [33]: Output current (a) and total harmonic distortion (b), and (c) Capacitors C1 and C2 voltages.

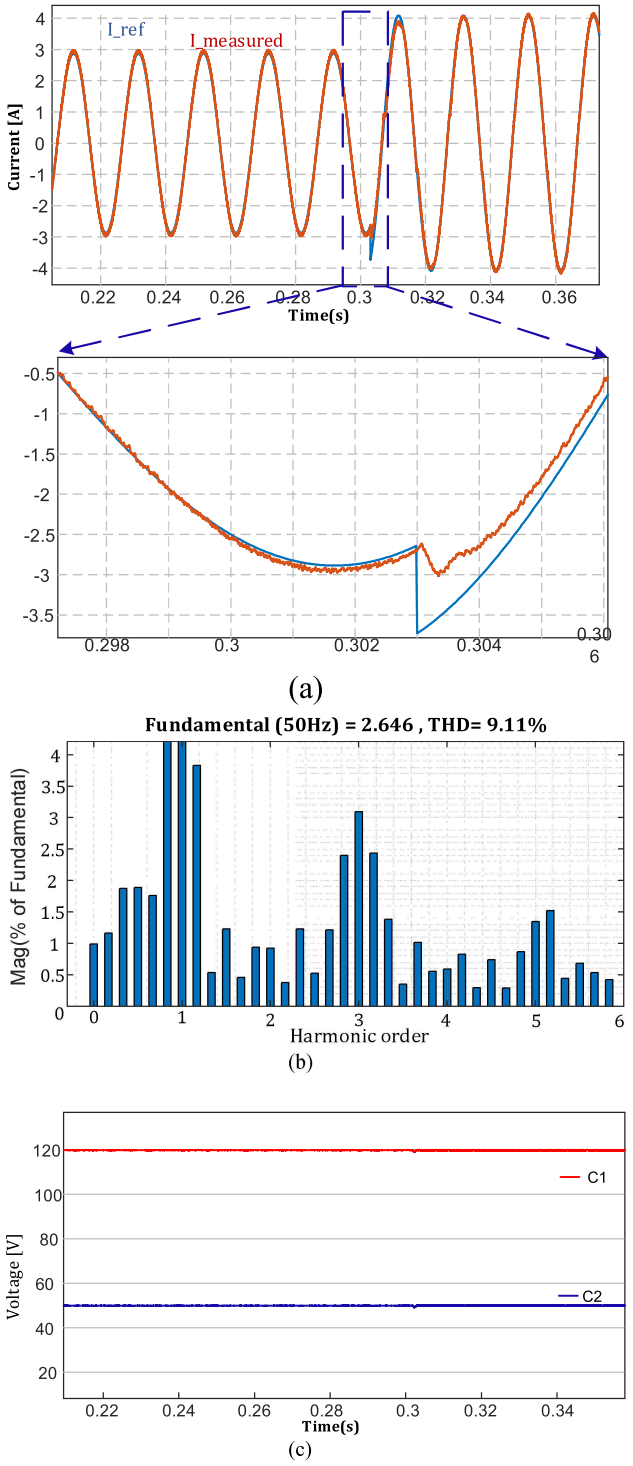

FIGURE 10. Case study #1 using proposed minimum loss MPC technique: Output current (a) and total harmonic distortion (b) and (c) Capacitors C1 and C2 voltages.

2 milliseconds. Besides, the behavior of the actual current at dynamic load for [33] has large overshoot, however it is small in the proposed technique.

In case study #1 the proposed technique demonstrated a THD around 9.11%, while Technique used in [33] demonstrated 11.7%.

Unbalanced load condition is tested to verify the ability fo the control system to handle unequal loading conditions, the results are displayed in Figure.11. The control system is following the reference and not widely affected by the unbalanced condition.

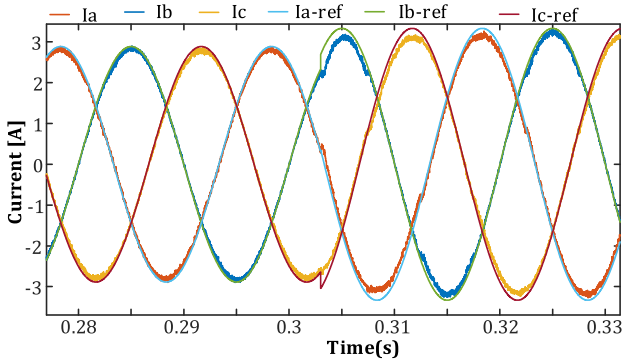

FIGURE 11. Unbalanced loading case of study, with Ra=12ohm, La=15mH, Rb=10 ohm, Lb=17mH and Ra=12ohm, La=13mH.

V. CONCLUSION

This work presented the control of the grid connected quasi Z-source converter using a modified model predictive control. The modified MPC algorithm was designed to eliminate the power losses of the quasi Z-source converter switches, inject a sinusoidal current into the grid and keep the balance of capacitors C1, and C2. The proposed algorithm was discussed in detail throughout the paper and to validate its performance comparative cases of the study were presented in the results section with similar MPC techniques and the obtained results showed that the proposed technique reduced the converter switches power losses by 10-20% based on the operating condition of each case of study.

FUTURE WORK

The research has several points suitable for future study, including the prediction horizon of the second or third higher degrees. In addition α, β, and γ are weighting factors, and they were chosen by trial and error. it is better to find an optimization method to choose these values. the trend towards working in a way that works online is the best.

REFERENCES

[1] *Statistical Review of World Energy 2021|70th edition in*. [Online]. Available: https://www.bp.com/content/dam/bp/business-sites/en/global/corporate/pdfs/energy-economics/statistical-review/bp-stats-review-2021-renewable-energy.pdf

[2] D. M. Said and K. M. Nor, "Effects of harmonics on distribution transformers," Presented at the Australas. Universities Power Eng. Conf. (AUPEC), Sydney, NSW, Australia, Dec. 2008.

[3] V. Oleschuk, M. Tirsu, V. Galbura, and I. Vasiliev, "Transformer-based PV system with modified techniques of PWM of diode-clamped inverters," in *Proc. Int. Conf. Develop. Appl. Syst. (DAS)*, May 2020, pp. 106–111, doi: 10.1109/DAS49615.2020.9108967.

[4] M. E. Ahmed, M. Orabi, and O. M. AbdelRahim, "Two-stage micro-grid inverter with high-voltage gain for photovoltaic applications," *IET Power Electron.*, vol. 6, no. 9, pp. 1812–1821, Nov. 2013, doi: 10.1049/iet-pel.2012.0666.

[5] M. Shayestegan, "Overview of grid-connected two-stage transformer-less inverter design," *J. Modern Power Syst. Clean Energy*, vol. 6, no. 4, pp. 642–655, Jul. 2018.

[6] H. Hachemi, A. Allali, and B. Belkacem, "Control of the power quality for a DFIG powered by multilevel inverters," *Int. J. Elect. Comput. Eng.*, vol. 10, no. 5, p. 4592, 2020.

[7] G. K. Srinivasan, M. Rivera, V. Loganathan, D. Ravikumar, and B. Mohan, "Trends and challenges in multi-level inverter with reduced switches," *Electronics*, vol. 10, no. 4, p. 368, Feb. 2021.

[8] H. Y. Ahmed, O. Abdel-Rahim, and Z. M. Ali, "High-gain seven-level switched-capacitor two-stage multi-level inverter," *Frontiers Energy Res.*, vol. 10, p. 462, May 2022, doi: 10.3389/fenrg.2022.869662.

[9] O. Abdel-Rahim and H. Wang, "Five-level one-capacitor boost multilevel inverter," *IET Power Electron.*, vol. 13, no. 11, pp. 2245–2251, Aug. 2020, doi: 10.1049/iet-pel.2020.0033.

[10] O. Abdel-Rahim, A. Chub, D. Vinnikov, and A. Blinov, "DC integration of residential photovoltaic systems: A survey," *IEEE Access*, vol. 10, pp. 66974–66991, 2022, doi: 10.1109/ACCESS.2022.3185788.

[11] C. R. Baier, F. A. Villarroel, M. A. Torres, M. A. Pérez, J. C. Hernández, and E. E. Espinosa, "A predictive control scheme for a single-phase grid-supporting quasi-Z-source inverter and its integration with a frequency support strategy," *IEEE Access*, vol. 11, pp. 5337–5351, 2023, doi: 10.1109/ACCESS.2023.3236499.

[12] S. Naderi and H. Rastegar, "A new non-isolated active quasi Z-source multilevel inverter with high gain boost," *IEEE Access*, vol. 11, pp. 2941–2951, 2023, doi: 10.1109/ACCESS.2023.3234040.

[13] N. Noroozi and M. R. Zolghadri, "Three-phase quasi-Z-source inverter with constant common-mode voltage for photovoltaic application," *IEEE Trans. Ind. Electron.*, vol. 65, no. 6, pp. 4790–4798, Jun. 2018, doi: 10.1109/TIE.2017.2774722.

[14] E. P. P. Soares-Ramos, L. De Oliveira-Assís, R. Sarrias-Mena, P. García-Triviño, C. A. García-Vázquez, and L. M. Fernández-Ramírez, "Averaged dynamic modeling and control of a quasi-Z-source inverter for wind power applications," *IEEE Access*, vol. 9, pp. 114348–114358, 2021, doi: 10.1109/ACCESS.2021.3104797.

[15] M. S. Endiz and R. Akkaya, "A modified quasi-Z-source inverter with enhanced performance capability," *Int. J. Renew. Energy Res.*, vol. 10, no. 2, pp. 892–897, Jun. 2020.

[16] O. Abdel-Rahim, A. Chub, H. M. Maheri, A. Blinov, and D. Vinnikov, "High-performance buck-boost partial power quasi-Z-source series resonance converter," *IEEE Access*, vol. 10, pp. 130177–130189, 2022, doi: 10.1109/ACCESS.2022.3225751.

[17] H. B. Dave, D. Singh, and H. O. Bansal, "High voltage gain reduced current ripple switched coupled inductor quasi-Z-source inverter," *Int. Trans. Electr. Energy Syst.*, vol. 30, no. 4, pp. 12305–12320, Apr. 2020.

[18] Y. Liu, X. Liu, X. Li, H. Yuan, and Y. Xue, "Model predictive control-based dual-mode operation of an energy-stored quasi-Z-source photovoltaic power system," *IEEE Trans. Ind. Electron.*, vol. 70, no. 9, pp. 9169–9180, Sep. 2023, doi: 10.1109/TIE.2022.3215451.

[19] X. Duan, L. Kang, H. Zhou, and Q. Liu, "Multivector model predictive power control with low computational burden for grid-tied quasi-Z-source inverter without weighting factors," *IEEE Trans. Power Electron.*, vol. 37, no. 10, pp. 11739–11748, Oct. 2022, doi: 10.1109/TPEL.2022.3174303.

[20] L. Guo, N. Jin, Y. Li, and K. Luo, "A model predictive control method for grid-connected power converters without AC voltage sensors," *IEEE Trans. Ind. Electron.*, vol. 68, no. 2, pp. 1299–1310, Feb. 2021, doi: 10.1109/TIE.2020.2970638.

[21] E. Kabalci and A. Boyar, "Highly efficient interleaved solar converter controlled with extended Kalman filter MPPT," *Energies*, vol. 15, no. 21, p. 7838, 2022, doi: 10.3390/en15217838.

[22] S. Zhuo, A. Gaillard, L. Xu, D. Paire, and F. Gao, "Extended state observer-based control of DC–DC converters for fuel cell application," *IEEE Trans. Power Electron.*, vol. 35, no. 9, pp. 9923–9932, Sep. 2020, doi: 10.1109/TPEL.2020.2974556.

[23] I. Poonahela, S. Bayhan, H. Abu-Rub, M. M. Begovic, and M. B. Shadmand, "An effective finite control set-model predictive control method for grid integrated solar PV," *IEEE Access*, vol. 9, pp. 144481–144492, 2021, doi: 10.1109/ACCESS.2021.3122325.

[24] J. K. Singh, K. A. Jaafari, R. K. Behera, K. A. Hosani, and U. R. Muduli, "Faster convergence controller with distorted grid conditions for photovoltaic grid following inverter system," *IEEE Access*, vol. 10, pp. 29834–29845, 2022, doi: 10.1109/ACCESS.2022.3159476.

[25] L. Tarisciotti, L. Chen, S. Shao, T. Dragicevic, P. Wheeler, and P. Zanchetta, "Finite control set model predictive control for dual active bridge converter," *IEEE Trans. Ind. Appl.*, vol. 58, no. 2, pp. 2155–2165, Mar. 2022, doi: 10.1109/TIA.2021.3135373.

[26] S. M. Akbar, A. Hasan, A. J. Watson, and P. Wheeler, "Model predictive control with triple phase shift modulation for a dual active bridge DC–DC converter," *IEEE Access*, vol. 9, pp. 98603–98614, 2021, doi: 10.1109/ACCESS.2021.3095553.
[27] F. Lin, X. Zhang, X. Li, C. Sun, W. Cai, and Z. Zhang, "Automatic triple phase-shift modulation for DAB converter with minimized power loss," *IEEE Trans. Ind. Appl.*, vol. 58, no. 3, pp. 3840–3851, May 2022, doi: 10.1109/TIA.2021.3136501.
[28] X. Yang, Y. Lyu, K. Wang, U. Kim, Z. Zhang, and K. Park, "A computationally efficient FCS-MPC imitator for grid-tied three-level NPC power converters based on sequential artificial neural network," in *Proc. IEEE Energy Convers. Congr. Expo. (ECCE)*, Oct. 2022, pp. 1–6, doi: 10.1109/ECCE50734.2022.9947831.
[29] I. S. Mohamed, S. Rovetta, T. D. Do, T. Dragicević, and A. A. Z. Diab, "A neural-network-based model predictive control of three-phase inverter with an output *LC* filter," *IEEE Access*, vol. 7, pp. 124737–124749, 2019, doi: 10.1109/ACCESS.2019.2938220.
[30] A. Bakeer, I. S. Mohamed, P. B. Malidarreh, I. Hattabi, and L. Liu, "An artificial neural network-based model predictive control for three-phase flying capacitor multilevel inverter," *IEEE Access*, vol. 10, pp. 70305–70316, 2022, doi: 10.1109/ACCESS.2022.3187996.
[31] D. Wang, Z. J. Shen, X. Yin, S. Tang, X. Liu, C. Zhang, J. Wang, J. Rodriguez, and M. Norambuena, "Model predictive control using artificial neural network for power converters," *IEEE Trans. Ind. Electron.*, vol. 69, no. 4, pp. 3689–3699, Apr. 2022, doi: 10.1109/TIE.2021.3076721.
[32] X. Yang, K. Wang, J. Kim, and K.-B. Park, "Artificial neural network-based FCS-MPC for three-level inverters," *J. Power Electron.*, vol. 22, no. 12, pp. 2158–2165, Dec. 2022, doi: 10.1007/s43236-022-00535-6.
[33] A. Bakeer, M. A. Ismeil, and M. Orabi, "Modified finite control set-model predictive controller (MFCS-MPC) for quasi Z-source inverters based on a current observer," *J. Power Electron.*, vol. 17, no. 3, pp. 610–620, May 2017.

MOHAMED A. ISMEIL (Member, IEEE) was born in Qena, Egypt, in October 1977. He received the B.Sc. and M.Sc. degrees in electrical engineering from South Valley University, in 2002 and 2008, respectively, and the dual Ph.D. degree from Aswan University and Technical University of Munich, Germany, in April 2014. From October 2010 to January 2013, he was a Ph.D. Student with the Channel System Program, Department of Electrical Drive Systems and Power Electronics, Technical University of Munich. From April 2014 to September 2018, he was an Assistance Professor with the Aswan Faculty of Engineering, Aswan University. Since October 2018, he has been an Associate Professor with the Faculty of Engineering, South Valley University, Qena. From March 2020 to 2022, he was the Head of the Electrical Department, Faculty of Engineering, Qena. He is currently an Associate Professor with the College of Engineering, King Khalid University, Saudi Arabia. He is also a member of the Aswan Power Electronics Applications Research Center (APEARC). He has published more than 45 papers in international conferences and journals. His current research interests include power electronics applications in wind energy conversion systems, PV interface with the utility, smart grid technologies, digital control application (PIC, FPGA, and DSP), and power inverter design for renewable applications.

OMAR ABDEL-RAHIM (Senior Member, IEEE) received the bachelor's and master's degrees in electrical engineering from the Faculty of Engineering, Aswan University, Aswan, Egypt, in 2009 and 2012, respectively, and the Ph.D. degree from Utsunomiya University, Japan, in 2017. From 2009 to 2012, he was a Research Assistant with the Aswan Power Electronic Application Research Center (APEARC). Since 2010, he has been with Aswan University, where he was an Assistant Lecturer with the Department of Electrical Engineering, Aswan Faculty of Engineering. In 2012, he joined Texas A&M University at Qatar, as a Research Associate. From 2017 to 2019, he was an Assistant Professor with the Faculty of Engineering, Aswan University, and the Vice-President of the Quality Assurance Unit, Faculty of Engineering, Aswan University. From 2018 to 2019, he was the Director of the APEARC. From 2018 to 2019, he was with the Power Electronics and Renewable Energy Laboratory (PEARL), ShanghaiTech University, Shanghai, China. From March 2021 to December 2022, he was a Postdoctoral Fellow with the Power Electronics Group, Tallinn University of Technology. He is currently an Assistant Professor with the Egypt-Japan University of Science and Technology, Egypt. He has authored or coauthored over 49 papers in leading international conferences and journals, mainly on the topics of grid connected inverters and multiphase matrix converter. His current research interests include multiphase machines drives, predictive control, renewable energy, smart grids, and dc–ac converters. He is a member of IES, IAS, PES, PELS, and IEEJ. He serves extensively as a reviewer for various IEEE/IET transactions and journals on power, electronics, circuits, and control engineering and several conferences.

HANY S. HUSSEIN (Senior Member, IEEE) received the B.Sc. degree in electrical engineering and the M.Sc. degree in communication and electronics from South Valley University, Egypt, in 2004 and 2009, respectively, and the Ph.D. degree in communication and electronics engineering from the Egypt-Japan University of Science and Technology (E-JUST), in 2013. In 2012, he was a Special Research Student with Kyushu University, Japan. He has been an Associate Professor with the Faculty of Engineering, Aswan University, since 2019. He is currently an Assistant Professor with the College of Engineering, King Khalid University, Saudi Arabia. His research interests include digital signal processing for communications, multimedia, image, and video coding, low-power wireless communications, one-bit ADC multiple-input multiple-output, underwater communication, index and spatial modulation, Li-Fi technology, and visible light communication. He is a technical committee member of many international conferences and a reviewer of many international conferences, journals, and transactions. Moreover, he was the General Co-Chair of the IEEE ITCE, in 2018.

ESAM H. ABDELHAMEED received the B.Sc. and M.Sc. degrees in electrical engineering from Minia University, Egypt, in 1997 and 2002, respectively, and the Ph.D. degree from the Nagoya Institute of Technology, Nagoya, Japan. He was a Postdoctoral Fellow with the Nagoya Institute of Technology, from March 2014 to August 2014. From September 2014 to July 2015, he was an Invited Researcher with the Nagoya Institute of Technology. He was a Researcher with the Mechanical Science and Engineering Department, Nagoya University, Nagoya, from August 2015 to March 2016. He is currently an Associate Professor with the Faculty of Energy Engineering, Aswan University, Egypt. His current research interests include applications of control theory and intelligent techniques to power system control and renewable energy.